

INVERSE KINEMATICS, FORWARD KINEMATICS AND WORKING SPACE DETERMINATION OF 3DOF PARALLEL MANIPULATOR WITH S-P-R JOINT STRUCTURE

Vladimir LUKANIN

Department of Manufacturing Engineering
Budapest University of Technology and Economics
H-1521 Budapest, Hungary
e-mail: v_lukanin@yahoo.com

Received: March 30, 2004

Abstract

This paper addresses the analysis of inverse kinematics, forward kinematics solutions and working space determination for the 3 degree-of-freedom (DOF) parallel manipulator with the S-P-R (Spherical-Prismatic-Revolute) joint structure. An effective approach is developed for the solution of inverse kinematics task in analytical form for given end-effector position. A method for working space determination which uses numerical solution of forward kinematics task is presented.

Keywords: parallel manipulators, S-P-R joint structure, inverse kinematics, working space.

1. Introduction

A wide variety of modern technologies need new types of tools and equipment. The requirements of a high accuracy and at the same time of high speed of production lead to development of new kinds of equipment and accessories in industry. This paper is dedicated to the parallel manipulators. This type of manipulators is well known and potentially able to perform even the functions of machine tools, and has the advantages of higher speed when precision kept.

The structure of manipulator known as Stewart platform was introduced by STEWART [1] in the middle of 1960^s for the simulation of flight conditions. The tyre-testing machine designed by GOUGH [2] also has parallel structure. The usage of in-parallel actuated mechanisms for the manipulating tasks was suggested by HUNT [3]. In the bibliographical oeuvre of BHASKAR [12] more than two hundreds publications linked with the different aspects of parallel manipulators are mentioned.

The present paper is dedicated to the 3-DOF manipulator with S-P-R structure which is not deeply studied in the literature. Only the manipulator (3-DOF, R-P-S) reviewed in [4, 5, 6] has illusive sameness with it. The R-P-S manipulator has the similar set of joints, but its order in parallel chains differs.

2. The Structure of Manipulator

During the work on the development of 3DOF parallel manipulator with the intersecting legs axes the fact that the unit of moving platform has essential drawbacks has led me to suggest a new type of construction. It is difficult to realize this unit providing a wide range of rotation angles, at the same time with desirable high precision and stiffness. So, a different type of kinematical structure was suggested. *Fig. 1* presents its principal construction:

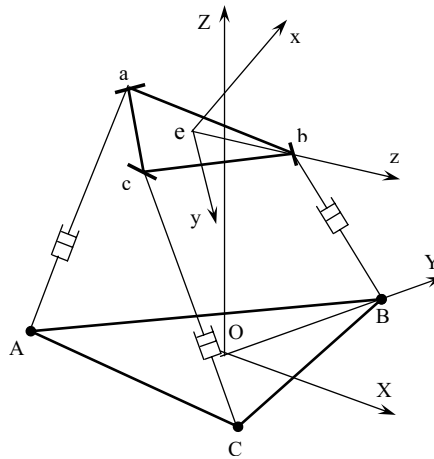


Fig. 1. Suggested structure of 3-DOF parallel manipulator

The moving platform (upper regular triangle) has 3 rotational joints located in the vertexes. The base platform is kept: it has the shape of a regular triangle with 3 spherical joints in corners. It is clear that this modification invokes the sophistication of the inverse and forward kinematics tasks solution. As it will be explained later, the forward kinematics task is solved numerically and the solution of inverse task is more complex. The manipulator with interferential legs has a simple solution of both tasks.

Below the solution for forward and inverse kinematics task is investigated. Using the results it is possible to control this parallel manipulator. Reviewing the materials of other researchers, we have found constructions with cosimilar structure. It has an inverse platform location, that is, revolute joints are on the base platform and spherical joints are on the moving one. Comparing the characteristics of both manipulators we have found that $3 \times (S-P-R)$ structure has bigger working volume. In the next parts of this paper the working zones of both cases are analyzed.

The kinematical structure of this type of manipulator is illustrated in *Fig. 2*.

We can estimate the working space of this manipulator in the following manner. Let us define the constraints imposed by each R-P-S chain. It is simple to illustrate our reasoning using top views of the base platform. The corresponding

figure is presented in the Appendix 1 (it illustrates constraint imposed by leg Aa, analogically might be described constraints imposed by two remaining legs). It is clear that for each leg this limitation of moving platform central point position can be described like the part of 3D space between two vertical planes (lines ρ on the figures representing top views) equidistant from the corresponding median of the base platform regular triangle. The distance from median to these planes is r , where r is the circumradius of moving platform triangle.

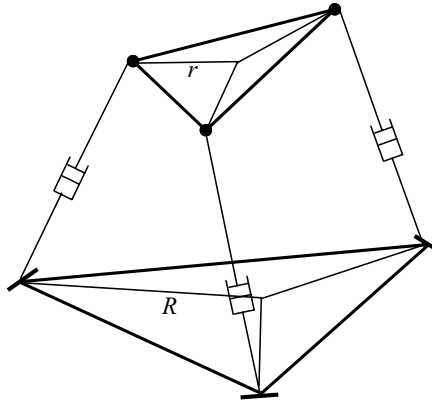


Fig. 2. 3 DOF parallel manipulator with R-P-S joint structure

As established by our simplified analysis, the work space of the R-P-S structure manipulator is principally limited in the X and Y directions (XY is the plane of base platform). As illustrated by *Fig. 3*, the resulting area is a regular hexagon with a centre equal to the centre of base platform (in 3D it is corresponding to the prism with vertical faces and hexagonal base).

This limitation is independent of the maximal length provided by the prismatic joints. From the detailed and exact analysis performed in [6] the working volume is limited by the cylinder with a radius equal to r .

It seems to us, by the reason of this limitation of R-P-S manipulator in X and Y directions, the S-P-R structure will have advantage in working space. That is to say, reviewing two manipulators (R-P-S and S-P-R) with the same maximal length provided by prismatic joints and equal platforms sizes, the S-P-R structure is promising to be preferable in sense of a bigger reachable space. This observation was the starting point for the analysis of 3 DOF parallel manipulator with S-P-R joint structure.

3. The Inverse Kinematics Task Solution

The 3-DOF parallel manipulator with S-P-R joint structure is shown in *Fig. 1*. This structure consists of two platforms which are schematically traced by triangles

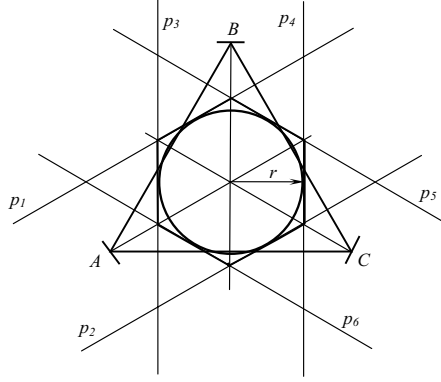


Fig. 3. Estimation of workspace as a superposition of three R-P-S chain constraints (top view)

abc and ABC, and three extensible links are shown by straight-line segments (Aa, Bb, Cc) each of them is connected to the upper (moving) platform by a rotational kinematical pair and to the base platform by a spherical one. The rotational pair axes are parallel to the opposite edges of the upper platform triangle.

Let us consider that manipulator end-effector is placed in the center point of the abc triangle (e point) and has the (X, Y, Z) coordinates in the base coordinate frame centered in O point.

So, the coordinates of base triangle vertexes:

$$\begin{aligned} X_A &= -\frac{\sqrt{3}}{2}R, & Y_A &= -\frac{R}{2}, & Z_A &= 0, \\ X_B &= 0, & Y_B &= R, & Z_B &= 0, \\ X_C &= \frac{\sqrt{3}}{2}R, & Y_C &= -\frac{R}{2}, & Z_C &= 0. \end{aligned} \quad (1)$$

The expressions for end-effector position coordinates are:

$$X = \frac{(X_a + X_b + X_c)}{3}, \quad Y = \frac{(Y_a + Y_b + Y_c)}{3}, \quad Z = \frac{(Z_a + Z_b + Z_c)}{3}.$$

These expressions together with the set of Eqs. (2)–(7) form the set of mechanical constraints.

$$(X - X_a)^2 + (Y - Y_a)^2 + (Z - Z_a)^2 = r^2 \quad (2)$$

$$(X - X_b)^2 + (Y - Y_b)^2 + (Z - Z_b)^2 = r^2 \quad (3)$$

$$(X - X_c)^2 + (Y - Y_c)^2 + (Z - Z_c)^2 = r^2 \quad (4)$$

$$-X_b(X_c - X_a) + (R - Y_b)(Y_c - Y_a) - Z_b(Z_c - Z_a) = 0 \quad (5)$$

$$\left(R \frac{\sqrt{3}}{2} + X_a\right)(X_b - X_c) + \left(\frac{R}{2} + Y_a\right)(Y_b - Y_c) + Z_a(Z_b - Z_c) = 0 \quad (6)$$

$$\left(R \frac{\sqrt{3}}{2} - X_c\right)(X_b - X_a) - \left(\frac{R}{2} + Y_c\right)(Y_b - Y_a) - Z_c(Z_b - Z_a) = 0. \quad (7)$$

Eqs. (2), (3), (4) describe the equidistant (to the vertexes) position of center point of the triangle. Eqs. (5), (6), (7) show that each of links (Aa, Bb, Cc) is perpendicular to the opposite edge of the platform triangle (cb, ac, ab). R and r are the radii of the circumscribed circles for the base and moving platform triangles, respectively.

Using the notion of φ, θ, ψ angles rotations from [8].

$$\begin{aligned} & R_{\varphi, \theta, \psi} R_{z, \varphi} R_{y, \theta} R_{x, \psi} \\ &= \begin{pmatrix} \cos(\varphi) & -\sin(\varphi) & 0 \\ \sin(\varphi) & \cos(\varphi) & 0 \\ 0 & 0 & 1 \end{pmatrix} \begin{pmatrix} \cos(\theta) & 0 & \sin(\theta) \\ 0 & 1 & 0 \\ -\sin(\theta) & 0 & \cos(\theta) \end{pmatrix} \\ &\quad \times \begin{pmatrix} 1 & 0 & 0 \\ 0 & \cos(\psi) & -\sin(\psi) \\ 0 & \sin(\psi) & \cos(\psi) \end{pmatrix} \quad (8) \\ &= \begin{pmatrix} \cos \varphi \cos \theta & \cos \varphi \sin \theta \sin \psi - \sin \varphi \cos \psi & \cos \varphi \sin \theta \cos \psi + \sin \varphi \sin \psi \\ \sin \varphi \cos \theta & \sin \varphi \sin \theta \sin \psi + \cos \varphi \cos \psi & \sin \varphi \sin \theta \cos \psi - \cos \varphi \sin \psi \\ -\sin \theta & \cos \theta \sin \psi & \cos \theta \cos \psi \end{pmatrix} \end{aligned}$$

Vectors of vertexes of moving platform in own coordinate frame:

$$\overline{ea} = \begin{vmatrix} 0 \\ -\frac{\sqrt{3}r}{2} \\ r \\ -\frac{r}{2} \end{vmatrix}, \quad \overline{eb} = \begin{vmatrix} 0 \\ 0 \\ r \end{vmatrix}, \quad \overline{ec} = \begin{vmatrix} 0 \\ \frac{\sqrt{3}r}{2} \\ \frac{r}{2} \\ -\frac{r}{2} \end{vmatrix}. \quad (9)$$

The position of the point of the moving platform in the base coordinate system is described by the equation:

$$\rho_{wc} = \rho_e + R\rho_{mc}, \quad (10)$$

where

- ρ_{wc} – the vector of point in the base coordinate frame,
- ρ_e – the vector of the moving coordinates system originating in the base coordinate frame,
- R – the rotational transformation matrix, ($R = \text{Rot}(z, \varphi)\text{Rot}(y, \theta), \text{Rot}(x, \psi)$).
- ρ_{mc} – the vector of point coordinates in the moving coordinate system.

Substituting (8) and (9) into (10) and considering notation $\rho_e = \begin{vmatrix} X \\ Y \\ Z \end{vmatrix}$ result

can be rewritten for each of the 9 coordinates (see Appendix 2).

Let us use the following transformation:

$$\begin{aligned} X_a &= X - X_1 + X_2, & Y_a &= Y - Y_1 + Y_2, & Z_a &= Z - Z_1 + Z_2, \\ X_b &= X - 2X_2, & Y_b &= Y - 2Y_2, & Z_b &= Z - 2Z_2, \\ X_c &= X + X_1 + X_2, & Y_c &= Y + Y_1 + Y_2, & Z_c &= Z + Z_1 + Z_2. \end{aligned} \quad (11)$$

Using the next notations:

$$\begin{aligned} X_1 &= (\cos \varphi \sin \theta \sin \psi - \sin \varphi \cos \psi) \frac{\sqrt{3}}{2} r, \\ X_2 &= -(\cos \varphi \sin \theta \cos \psi + \sin \varphi \sin \psi) \frac{r}{2}, \\ Y_1 &= (\sin \varphi \sin \theta \sin \psi + \cos \varphi \cos \psi) \frac{\sqrt{3}}{2} r, \\ Y_2 &= -(\sin \varphi \sin \theta \cos \psi - \cos \varphi \sin \psi) \frac{r}{2}, \\ Z_1 &= \cos \theta \sin \psi \frac{\sqrt{3}}{2} r, \\ Z_2 &= -\cos \theta \cos \psi \frac{r}{2}. \end{aligned} \quad (12)$$

It is possible to simplify the set of constraint Eqs. (2)–(7), and the simplified equations set can be presented in the following form:

$$\begin{cases} X_1^2 + Y_1^2 + Z_1^2 &= \frac{3}{4} r^2 \\ X_2^2 + Y_2^2 + Z_2^2 &= \frac{1}{4} r^2 \\ X_1 X_2 + Y_1 Y_2 + Z_1 Z_2 &= 0 \\ R Y_1 + \sqrt{3} R X_2 &= 0 \\ -2X X_1 - 3R \sqrt{3} X_2 + (-R - 2Y) Y_1 - 2Z Z_1 &= 0 \\ -R \sqrt{3} X_1 - 6X X_2 + (-3R - 6Y) Y_2 - 6Z Z_2 &= 0 \end{cases} \quad (13)$$

Now it is possible to analyze how to solve this system of equations. From the 4th equation we can define the following expression for one of the variables:

$$\varphi = \arctan(\tan^{-1}(\psi)). \quad (14)$$

Then using this result and rewriting the equation set in a form with the φ, θ, ψ angles as variables we can receive the analytical solution applying the *Maple symbolic*

calculation program. Note that it is necessary to solve only the last two equations of (13), because the first tree equations are meaningless (these equations with substitution of φ, θ, ψ angles are transformed in equalities). The solution is shown in Appendix 3. The second equation from the resulting set defines the ψ angle, and it can be rewritten the following form:

$$A4 \tan^4(\psi) + A3 \tan^3(\psi) + A2 \tan^2(\psi) + A1 \tan(\psi) + A0 = 0,$$

where

$$\begin{aligned} A4 &= 4Z^2Y^2 + 4X^2RY + 4Z^2RY + X^2R^2 + 4X^2Y^2; \\ A3 &= 8Y^3X - 8X^3Y - 4XRZ^2 - 8XYZ^2 - 4RY^2X - 4X^3R - 4R^2YX; \\ A2 &= -2X^2R^2 + 4Z^2Y^2 + 4Z^2X^2 - 12Z^2RY + 4Y^2R^2 + 4Y^4 + 4X^4 \\ &\quad - 16X^2Y^2 - 8Y^3R; \\ A1 &= 8X^3Y + 12XRZ^2 - 8XYZ^2 - 8Y^3X + 4X^3R + 4RY^2X + 4R^2YX; \\ A0 &= X^2R^2 + 4Z^2X^2 + 4X^2RY + 4X^2Y^2. \end{aligned} \tag{15}$$

It is the 4th order polynomial of $\tan(\psi)$ variable. Relation (15) presents the main result. The resolution of this polynomial will be the most time consuming procedure in the algorithm realizing calculation for considering the manipulator structure inverse kinematics problem. It is known that it is possible to solve this polynomial analytically. Only few steps remain: a) evaluate φ using (14); b) from the first equation of Appendix 3 it is possible to determine θ ; c) verification of all existing triads (φ, θ, ψ). The common solution of the polynomial (15) was produced also by the symbolic 'calculator' like a function of 5 parameters (the coefficients of polynomial), and the C program code was generated for the next usage in the modelling program. The formula for one of the four roots of Eq. (15) is shown in Appendix 4.

Note that (15) represents the solution of the general case X, Y, Z . The full solution of the inverse kinematics task also comprises a set of solutions in special cases defined by specific locations of end-effector as follows:

$$\begin{aligned} &\{X = 0, Y = 0, \theta = -\pi/2, \varphi = \arctan(1/\tan(\psi))\}, \\ &\{X = 0, Y = R, \theta = \pi/2, \varphi = \pm\pi/4, \psi = \pm\pi/4\}, \\ &\left\{ \begin{aligned} &X = \pm\sqrt{3}Y, \varphi = \arctan(\pm 1/\sqrt{3}), \\ &\psi = \arctan(\pm\sqrt{3}), Z = \pm \frac{R + R \sin(\theta) - 4Y \sin(\theta)}{2 \cos(\theta)} \end{aligned} \right\}, \tag{16} \\ &\left\{ \psi = \arctan \left(\pm \sqrt{\pm \frac{-1 + 3a + 2\sqrt{-2a + 2a^2}}{1 + a}} \right), \right. \\ &\quad \left. (a = R/Y), \theta = \pi/2, \varphi = \arctan(1/\tan(\psi)0) \right\} \end{aligned}$$

4. Modelling and Numerical Results

The code of calculation φ, θ, ψ angles by formulas described above for the specified X, Y, Z is the base of this model and of the method of verification. Note that this code was generated by the Maple program. In Appendix 3 the code for the first root of the 4th order polynomial is shown. It can be clearly recognized that for the robot control systems application it will be very useful to optimize this code, because it contains many repetitive parts. Only the pre-calculation with the substitution of the next numerical values substitution instead of evaluating the complicated expressions reduces essentially the calculation cost of this part of algorithm (this optimization procedure is also provided by Maple).

Then corresponding to the formulas (12), $X_1, X_2, Y_1, Y_2, Z_1, Z_2$ values are calculated, and finally, using Eq. (11) the coordinates of the moving platform triangle vertexes are defined.

There are 8 manipulator poses in Fig. 4 which correspond to all the possible solutions for the present kinematical structure with parameters generated randomly by a computer. The norm of correctness of the inverse kinematics task solution is the fact that each dot product of vector of leg and corresponding vector of revolute joint axis is infinitesimal. During the huge number of trials with different positions of end-effector and different ratios R/r the value of this norm has the order of $10^{-15} - 10^{-20}$ which can be recognized as round-off error of computer calculations.

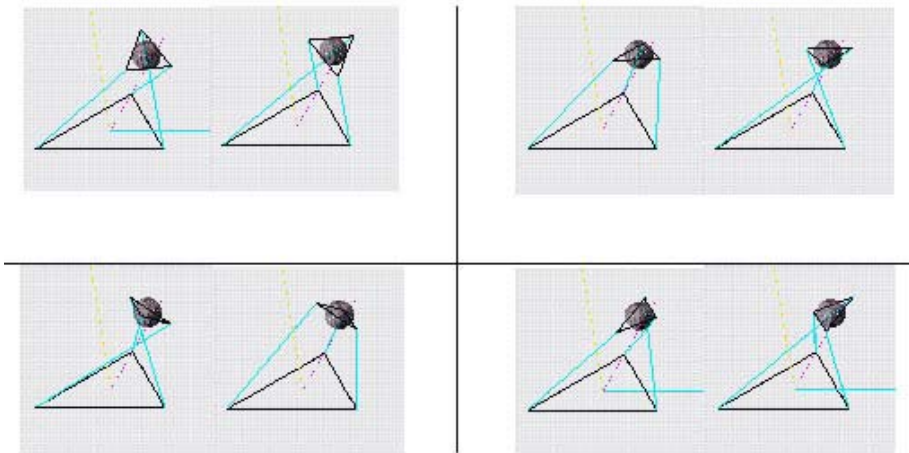


Fig. 4. All solutions of the inverse kinematics task ($R = 142, r = 50, X = 75.54, Y = 47.23, Z = 129.34$)

5. Forward Kinematics Task Solution

Let us consider the forward kinematics task of the 3DOF S-P-R parallel manipulator. The task is to find the X, Y, Z coordinates of e point (see Fig. 1) when the legs lengths l_1, l_2, l_3 are known. As it will be shown in the following reasoning, it is possible to describe the convenient mathematical model for the manipulator R-P-S with the corresponding platform sizes and l_1, l_2, l_3 parameters, and solve numerically the forward kinematics for it using the angles of revolute joints as variables, then it is possible to perform the uniquely defined transformation, which allows to determine the X, Y, Z parameters of the corresponding S-P-R structure. In other words it is equivalent if we reviewed the structure considering the platforms first as the base and second as moving and vice versa.

Let us consider the R-P-S structure (Fig. 5)

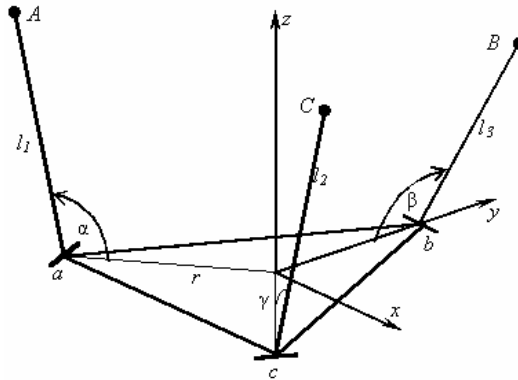


Fig. 5. The R-P-S joint structure with angles α, β, γ

The set of geometrical constraints for the case of R-P-S manipulator is the $|AB| = |BC| = |CA| = \sqrt{3}R$. The mathematical model in this case is introduced by the following set of equations:

$$\begin{cases} (x_B - x_A)^2 + (y_B - y_A)^2 + (z_B - z_A)^2 = 3R^2 \\ (x_C - x_B)^2 + (y_C - y_B)^2 + (z_C - z_B)^2 = 3R^2 \\ (x_A - x_C)^2 + (y_A - y_C)^2 + (z_A - z_C)^2 = 3R^2 \end{cases} \quad (17)$$

Fig. 6 illustrates the determination of the A point coordinates. In similar manner it is possible to define the coordinates of B and C points.

So, the coordinates of the A, B and C points are:

$$\begin{aligned} x_A &= -r \frac{\sqrt{3}}{2} + \frac{\sqrt{3}}{2} l_1 \cos(\alpha), \\ y_A &= -\frac{r}{2} + \frac{1}{2} l_1 \cos(\alpha), \end{aligned}$$

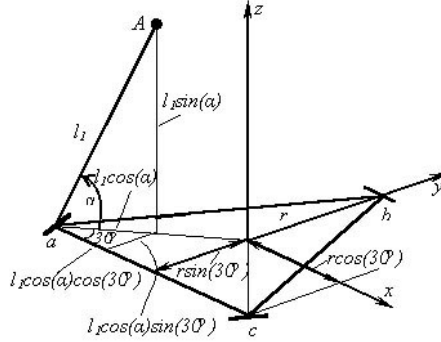


Fig. 6. The determination of the A point coordinates

$$\begin{aligned}
 z_A &= l_1 \sin(\alpha), \\
 x_B &= 0, \\
 y_B &= r - l_2 \cos(\beta), \\
 z_B &= l_2 \sin(\beta), \\
 x_C &= r \frac{\sqrt{3}}{2} - \frac{\sqrt{3}}{2} l_3 \cos(\gamma), \\
 y_C &= -\frac{r}{2} + \frac{1}{2} l_3 \cos(\gamma), \\
 z_C &= l_3 \sin(\gamma);
 \end{aligned} \tag{18}$$

Substituting (18) into (17) we can determine the mathematical model like a system of three equations non-linear relatively to the α, β, γ variables and with the l_1, l_2, l_3 parameters

$$\begin{cases} f_1(\alpha, \beta, \gamma) = 0 \\ f_2(\alpha, \beta, \gamma) = 0 \\ f_3(\alpha, \beta, \gamma) = 0, \end{cases} \tag{19}$$

where

$$\begin{aligned}
 f_1 &= \left(\frac{r\sqrt{3}}{2} - \frac{\sqrt{3}}{2} l_1 \cos(\alpha) \right)^2 + \left(\frac{3r}{2} - l_2 \cos(\beta) - \frac{l_1}{2} \cos(\alpha) \right)^2 \\
 &\quad + (l_2 \sin(\beta) - l_1 \sin(\alpha))^2 - 3R^2; \\
 f_2 &= \left(\frac{r\sqrt{3}}{2} - \frac{\sqrt{3}}{2} l_3 \cos(\gamma) \right)^2 + \left(-\frac{3r}{2} + l_2 \cos(\beta) + \frac{l_3}{2} \cos(\gamma) \right)^2 \\
 &\quad + (l_3 \sin(\gamma) - l_2 \sin(\beta))^2 - 3R^2;
 \end{aligned} \tag{20}$$

$$f_3 = \left(-r\sqrt{3} + \frac{\sqrt{3}}{2}l_1 \cos(\alpha) + \frac{\sqrt{3}}{2}l_3 \cos(\gamma) \right)^2 + \left(\frac{l_1 \cos(\alpha)}{2} - \frac{l_3 \cos(\gamma)}{2} \right)^2 + (l_1 \sin(\alpha) - l_3 \sin(\gamma))^2 - 3R^2;$$

and

$$\alpha \in [0, 2\pi[, \quad \beta \in [0, 2\pi[, \quad \gamma \in [0, 2\pi[.$$

It is possible to find the solution of this system numerically. We used the numerical procedure mentioned in the literature as Newton–Kantorovich method. This method is described in Appendix 5.

5.1. Implementation of the Newton-Kantorovich Method

As it is clear from the essentials of the method, it is necessary to determine the partial derivatives of component functions of the system (19) to define the set of equations of the numerical method iteration (A5.1):

$$A = \begin{vmatrix} \frac{\partial f_1}{\partial \alpha} & \frac{\partial f_1}{\partial \beta} & \frac{\partial f_1}{\partial \gamma} \\ \frac{\partial f_2}{\partial \alpha} & \frac{\partial f_2}{\partial \beta} & \frac{\partial f_2}{\partial \gamma} \\ \frac{\partial f_3}{\partial \alpha} & \frac{\partial f_3}{\partial \beta} & \frac{\partial f_3}{\partial \gamma} \end{vmatrix}.$$

The expressions for partial derivatives are the following:

$$\frac{\partial f_1}{\partial \alpha} = \frac{3}{2} (r - l_1 \cos(\alpha)) l_1 \sin(\alpha) + \left(\frac{3r}{2} - l_2 \cos(\beta) - \frac{l_1}{2} \cos(\alpha) \right) l_1 \sin(\alpha) - 2 (l_2 \sin(\beta) - l_1 \sin(\alpha)) l_1 \cos(\alpha);$$

$$\frac{\partial f_1}{\partial \beta} = 2 \left(\frac{3r}{2} - l_2 \cos(\beta) - \frac{l_1}{2} \cos(\alpha) \right) l_2 \sin(\beta) + 2 (l_2 \sin(\beta) - l_1 \sin(\alpha)) l_2 \cos(\beta);$$

$$\frac{\partial f_1}{\partial \gamma} = 0;$$

$$\frac{\partial f_2}{\partial \alpha} = 0;$$

$$\frac{\partial f_2}{\partial \beta} = 2 \left(\frac{3r}{2} - l_2 \cos(\beta) - \frac{l_3}{2} \cos(\gamma) \right) l_2 \sin(\beta) - 2 (l_3 \sin(\gamma) - l_2 \sin(\beta)) l_2 \cos(\beta);$$

$$\frac{\partial f_2}{\partial \gamma} = \frac{3}{2} (r - l_3 \cos(\gamma)) l_3 \sin(\gamma) + \left(\frac{3r}{2} - l_2 \cos(\beta) - \frac{l_3}{2} \cos(\gamma) \right) l_3 \sin(\gamma) + 2 (l_3 \sin(\gamma) - l_2 \sin(\beta)) l_3 \cos(\gamma);$$

$$\frac{\partial f_3}{\partial \alpha} = -\frac{3}{2} (l_1 \cos(\alpha) + l_3 \cos(\gamma) - 2r) l_1 \sin(\alpha) - \frac{1}{2} (l_1 \cos(\alpha) - l_3 \cos(\gamma)) l_1 \sin(\alpha) + 2 (l_1 \sin(\alpha) - l_3 \sin(\gamma)) l_1 \cos(\alpha);$$

$$\frac{\partial f_3}{\partial \beta} = 0;$$

$$\frac{\partial f_3}{\partial \gamma} = -\frac{3}{2} (l_1 \cos(\alpha) + l_3 \cos(\gamma) - 2r) l_3 \sin(\gamma) + \frac{1}{2} (l_1 \cos(\alpha) - l_3 \cos(\gamma)) l_3 \sin(\gamma) - 2 (l_1 \sin(\alpha) - l_3 \sin(\gamma)) l_3 \cos(\gamma);$$

In each iteration it is necessary to solve the system of linear *Eqs. (19)* which we can rewrite in the form $A(x^{(0)})z = -f(x^{(0)})$.

The system is solved using Cramer's determinants method. Let us determine the structure of corresponding matrixes and its determinants

The structure of matrix A will be the following:

$$A = \begin{vmatrix} a_{11} & a_{12} & 0 \\ 0 & a_{22} & a_{23} \\ a_{31} & 0 & a_{33} \end{vmatrix},$$

$$\text{Det}(A) = a_{11}a_{22}a_{33} + a_{31}a_{12}a_{23};$$

$$A_\alpha = \begin{vmatrix} -f_1(x^{(k)}) & a_{12} & 0 \\ -f_2(x^{(k)}) & a_{22} & a_{23} \\ -f_3(x^{(k)}) & 0 & a_{33} \end{vmatrix},$$

$$\text{Det}(A_\alpha) = -f_1(x^{(k)})a_{22}a_{33} + f_2(x^{(k)})a_{12}a_{33} - f_3(x^{(k)})a_{12}a_{23};$$

$$A_\beta = \begin{vmatrix} a_{11} & -f_1(x^{(k)}) & 0 \\ 0 & -f_2(x^{(k)}) & a_{23} \\ a_{31} & -f_3(x^{(k)}) & a_{33} \end{vmatrix},$$

$$\text{Det}(A_\beta) = -a_{11}f_2(x^{(k)})a_{33} + a_{11}a_{23}f_3(x^{(k)}) - a_{31}f_1(x^{(k)})a_{23};$$

$$A_\gamma = \begin{vmatrix} a_{11} & a_{12} & -f_1(x^{(k)}) \\ 0 & a_{22} & -f_2(x^{(k)}) \\ a_{31} & 0 & -f_3(x^{(k)}) \end{vmatrix},$$

$$\text{Det}(A_\gamma) = -a_{11}a_{22}f_3(x^{(k)}) - a_{31}a_{12}f_2(x^{(k)}) + a_{31}a_{22}f_1(x^{(k)});$$

$$\begin{aligned}
 a_{11} &= \frac{\partial f_1}{\partial \alpha}, & a_{12} &= \frac{\partial f_1}{\partial \beta}, & a_{13} &= \frac{\partial f_1}{\partial \gamma}; \\
 a_{21} &= \frac{\partial f_2}{\partial \alpha}, & a_{22} &= \frac{\partial f_2}{\partial \beta}, & a_{23} &= \frac{\partial f_2}{\partial \gamma}; \\
 a_{31} &= \frac{\partial f_3}{\partial \alpha}, & a_{32} &= \frac{\partial f_3}{\partial \beta}, & a_{33} &= \frac{\partial f_3}{\partial \gamma};
 \end{aligned}$$

And consequently, the solution for iteration $k + 1$ can be written as:

$$\begin{aligned}
 \alpha^{k+1} &= \text{Det}(A_\alpha) / \text{Det}(A) + \alpha^k; \\
 \beta^{k+1} &= \text{Det}(A_\beta) / \text{Det}(A) + \beta^k; \\
 \gamma^{k+1} &= \text{Det}(A_\gamma) / \text{Det}(A) + \gamma^k;
 \end{aligned}$$

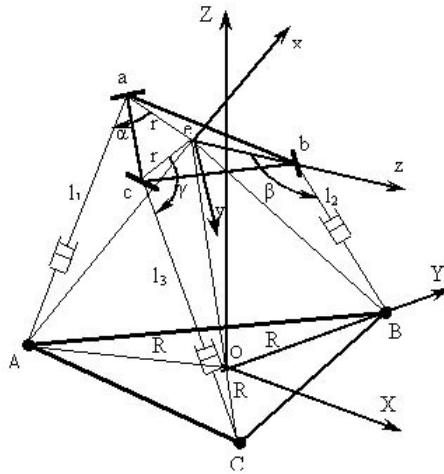


Fig. 7. The S-P-R structure manipulator

Supposing that initial estimation was chosen properly (close enough to the real solution of the system), this method after finite number of refinement iterations gives the numerical solution of the system (19) with the required accuracy. Then, it is necessary to implement the back transformation: we have to determine the corresponding end-effector position of the S-P-R structure manipulator.

Let us consider Fig. 7. It is clear that position of point e is defined as product of intersection of three spheres with radii $|Ae|$, $|Be|$, $|Ce|$ and centers in points A , B and C , respectively.

The radii of spheres can be determined from triangles Aea , Beb and Cec

using the cosine theorem:

$$\begin{aligned} |Ae|^2 &= l_{11}^2 = l_1^2 + r^2 - 2l_1r \cos(\alpha); \\ |Be|^2 &= l_{22}^2 = l_2^2 + r^2 - 2l_2r \cos(\beta); \\ |Ce|^2 &= l_{33}^2 = l_3^2 + r^2 - 2l_3r \cos(\gamma). \end{aligned} \quad (21)$$

The intersection of three spheres presented by the following system:

$$\begin{cases} (X - X_A)^2 + (Y - Y_A)^2 + (Z - Z_A)^2 = l_{11}^2, \\ (X - X_B)^2 + (Y - Y_B)^2 + (Z - Z_B)^2 = l_{22}^2, \\ (X - X_C)^2 + (Y - Y_C)^2 + (Z - Z_C)^2 = l_{33}^2, \end{cases}$$

and taking (1) into consideration we can rewrite it as follows:

$$\begin{cases} \left(X + \frac{\sqrt{3}}{2}R\right)^2 + \left(Y + \frac{R}{2}\right)^2 + Z^2 = l_{11}^2, \\ X^2 + (Y - R)^2 + Z^2 = l_{22}^2, \\ \left(X - \frac{\sqrt{3}}{2}R\right)^2 + \left(Y + \frac{R}{2}\right)^2 + Z^2 = l_{33}^2, \end{cases} \quad (22)$$

Solution of (22) with the additional condition $Z \geq 0$ is in the case of real manipulator:

$$\left\{ X = \frac{\sqrt{3}}{6R}(l_{11}^2 - l_{33}^2); Y = \frac{\sqrt{3}(l_{11}^2 + l_{33}^2 - 2l_{22}^2)}{6R}; Z = \sqrt{l_{22}^2 - X^2 - (Y - R)^2} \right\}. \quad (23)$$

6. Determination of Working Space

The determination of working space (WS) of manipulator is one of the most important tasks during the manipulator design, also for implementation of existing manipulators in concrete operations or processes.

We suggest estimating the WS of our manipulator in the following manner:

For each element of the big enough set of discrete manipulator configurations $(l_1, l_2, l_3)_1, \dots, (l_1, l_2, l_3)_n$ we should determine the corresponding robot end-effector positions $(X, Y, Z)_1 \dots (X, Y, Z)_m$. As described above, we can numerically solve this problem for each triad $(l_1, l_2, l_3)_j$. The following pseudo code presents the algorithm of working space determination:

```

procedure main_loop
for  $l_1 = l_{1 \min}$  to  $l_{1 \max}$  by step  $\Delta l_1$ 
for  $l_2 = l_{2 \min}$  to  $l_{2 \max}$  by step  $\Delta l_2$ 
for  $l_3 = l_{3 \min}$  to  $l_{3 \max}$  by step  $\Delta l_3$ 
{
    numerically_solve_forward_kinematics ( $l_1, l_2, l_3$ );
}

```

As it is clear from the manipulator construction we can assume that $l_{1\min} = l_{2\min} = l_{3\min}$, $l_{1\max} = l_{2\max} = l_{3\max}$ and $\Delta l_1 = \Delta l_2 = \Delta l_3$.

The cycle internal function should solve the forward kinematics task. Let us determine that the Newton–Kantorovich (N-K) method described above gives only a local solution. That is, implementing the algorithm for a given pose of manipulator $(l_1, l_2, l_3)_j$ and a given initial estimation of $\alpha_0, \beta_0, \gamma_0$ which iteratively performs calculations described by formulas (19) ... (23), we can determine the solution which is close to the chosen estimation, or in unfortunate cases the algorithm fails (the initial estimation is not appropriate). The solution of forward kinematics in $(l_1, l_2, l_3)_j$ gives the set of solutions. According to data published in [9] this set may contain up to 8 elements. So, we have to implement the local algorithm N-K for the set of initial estimations $(\alpha_0, \beta_0, \gamma_0)_1 \dots (\alpha_0, \beta_0, \gamma_0)_k$ and save the come off solutions erasing duplicates. I shall explain in the following lines which will be this set of estimations.

The structure of algorithm realizing the forward kinematics solution will be:

```

procedure numerically_solve_forward_kinematics ( $l_1, l_2, l_3$ )
{
  for  $\alpha_0 = 0$  to  $2\pi$  by step  $\Delta\alpha_0$ 
  for  $\beta_0 = 0$  to  $2\pi$  by step  $\Delta\beta_0$ 
  for  $\gamma_0 = 0$  to  $2\pi$  by step  $\Delta\gamma_0$ 
  {
    locally_solve_forward_kinematics ( $l_1, l_2, l_3, \alpha_0, \beta_0, \gamma_0$ );
  }
}

```

We have realized this algorithm. And for the parameters $R = 0.75$, $r = 0.25$, $l_{\min} = 0$, $l_{\max} = 1.0$ after a set of experiments the essential heuristics has been found: the whole set of $(X, Y, Z)_1 \dots (X, Y, Z)_m$ did not change if $\Delta\alpha = \Delta\beta = \Delta\gamma \leq (2\pi/5)$. Or in other words, the total number of steps in the internal cycles in numerically_solve_forward_kinematics procedure can be limited to as small as 5. Even more, in the case of 4 steps per cycle, 99.997% of elements $(X, Y, Z)_1 \dots (X, Y, Z)_m$ found in the case of 16 steps per cycle were determined. This fact allows highly decrease the time of calculations using proper density of search trial points in forward kinematics solution.

Also it is possible to effectively use the symmetry property of our manipulator. For example, if we solve numerically the forward kinematics task for robot configuration $(l_1, l_2, l_3)_k$ and find corresponding set of end-effector positions $\{(X, Y, Z)_1, \dots, (X, Y, Z)_p\}$ so, for the configurations which differ only in order of corresponding leg lengths but the values hold $((l_1, l_3, l_2), (l_2, l_1, l_3), (l_2, l_3, l_1), (l_3, l_1, l_2), (l_3, l_2, l_1))$, we do not need to solve the forward kinematics problem. It is possible to find the solutions for them using simple transformations in a Cartesian space.

If we consider the concrete configuration (l_1, l_2, l_3) and solve the forward kinematics task in this point and, consequently, we have the set of solutions $SS =$

$\{(X, Y, Z)_1, \dots, (X, Y, Z)_p\}$, so we can determine the solutions $SS' = \{(X, Y, Z)'_1, \dots, (X, Y, Z)'_p\}$ for case (l_2, l_3, l_1) applying the rotation around Z axis in base coordinate frame on angle 120° for each element of SS . The solutions $SS^* = \{(X, Y, Z)^*_1, \dots, (X, Y, Z)^*_p\}$ for configuration (l_3, l_2, l_1) can be determined by mirror imaging about the ZY plane. It is possible to prove rigorously the correctness of these transformations. And consequently, the remaining permutations (l_1, l_3, l_2) , (l_2, l_1, l_3) , (l_3, l_1, l_2) are also correct because each of them can be performed like a sequence of rotations and mirror imaging described above.

The schema in Appendix 6 shows the starting configuration (l_1, l_2, l_3) and the whole set of configurations which can be easily determined applying transformations in Cartesian space. In figure of Appendix 6 the configurations $((l_1, l_2, l_3), (l_2, l_3, l_1), (l_3, l_1, l_2), (l_3, l_2, l_1), (l_1, l_3, l_2), (l_2, l_1, l_3))$ are indicated by Roman numbers (I-VI) and the corresponding linkages between the configurations are denoted by the graphical signs (using sequence of rotational and mirror transformations we are able to generate one configuration from another). For example: we can reach the configuration II from I using rotation about Z axis by 120° counter-clockwise, V from I applying the mirror imaging about the vertical plane spanned by lines AO and OZ (or I->II and then by means of mirror transformation reach V), and so on.

The property of symmetry allows making a sufficient improvement of the proposed algorithm. Supposing that $\Delta l_1 = \Delta l_2 = \Delta l_3 = \Delta l$ and $l_{1\max} = l_{2\max} = l_{3\max} = l_{\max}$ the structure of main_loop procedure will be following:

```

procedure main_loop
for  $l_1 = l_{\min}$  to  $l_{1\max}$  by step  $\Delta l$ 
for  $l_2 = l_{\min}$  to  $l_1$  by step  $\Delta l$ 
for  $l_3 = l_{\min}$  to  $l_2$  by step  $\Delta l$ 
{
     $SS = \underline{\text{numerically\_solve\_forward\_kinematics}}(l_1, l_2, l_3);$ 
    transformations(SS);
}

```

Let us determine that in each cycle in main_loop procedure consists of N steps and consequently in the variant when we evaluate all steps in each cycle the total number of numerically_solve_forward_kinematics evaluations will be N^3 . After modification this number can be calculated according to the following formula:

$$N_{total_new} = \sum_{i=1}^N \sum_{j=1}^i \sum_{k=1}^j 1 = \frac{1}{6} ((N+1)^3 - N - 1),$$

Consequently, when the N is big enough, six times less evaluations of forward kinematics will be performed, and due to the fact that the transformations in Cartesian space are simple and have small computational cost, so, the whole time of computations is reduced approximately six times. Also the heuristics how to choose the proper initial estimations was found. Solving Eqs. (21) ... (23), we detected that

we should choose only the $(\alpha_0, \beta_0, \gamma_0)_i$ which gave a real number solution (23), concretely, the radicand in the expression for Z should be non-negative.

For both cases: S-P-R and R-P-S manipulators with parameters $R = 0.75$ (base platform), $r = 0.25$ (moving platform), $l_{\min} = 0$, $l_{\max} = 1.0$ the working space is presented in Fig. 8. The cylinder of $r = 0.25$ is the estimation of working space for R-P-S manipulator (in the top part it should be edged to the point of vertex of working space for S-P-R).

The supposition that S-P-R structure has a bigger working space volume now has been confirmed.

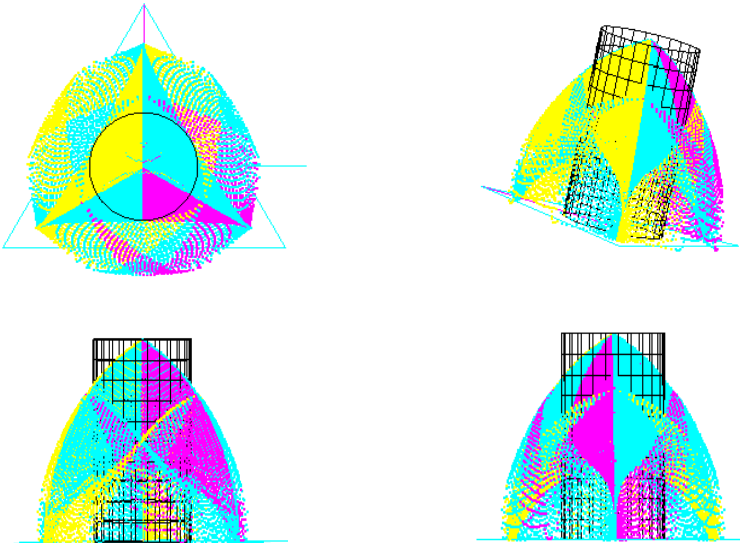


Fig. 8. The working space of S-P-R and R-P-S manipulators

7. Conclusions

The special aspects of 3DOF parallel manipulator with S-P-R joint structure had been investigated. Interesting results of usage of the local method of Newton for the global problem was shown. It does not mean that this style is appropriate in a general case, but for the problem of working space determination of the described manipulator it is good enough. The system of non-linear equations (the system of geometrical constraints for forward kinematics in our case) can be reviewed as a global optimization problem. The general methods described in literature for the solution of a global optimization problem [10], [11] have ‘bottlenecks’. For example, these methods have slow convergency in close vicinity of solution,

and consequently to implement them for the forward kinematics solution it was necessary to include the local method in the algorithm (the algorithm should be hybrid ‘global-local’ to find solutions with appropriate accuracy). Also there are difficulties to determine some numerical parameters to implement the Lipschitz optimization algorithms of [10], the algorithm suggested in [11] has a much more complicated program realization comparing with the one suggested by us. As an interesting fact was established that the simultaneous development of algorithms for the forward kinematics task solution and working space determination has allowed making improvements and modifications in both algorithms.

The methods described in this paper give good practical results and can be used during the development of this type of manipulators. The advantages of 3 DOF manipulator of S-P-R structure comparing with the case of R-P-S were also illustrated and explained. Only simple modifications can be implemented in the presented methodology for the case of S-P-R manipulator which has the end-effector on the normal to the moving platform triangle crossing it in the center.

Acknowledgements

I would like to express thanks to OTKA of the Hungarian Academy of Sciences (OTKA TO 37225) and to the Hungarian Ministry of Education for the support of the doctoral program in frame of which this research was conducted. Special thanks are due to my supervisor Dr. János Somló and Dr. Mátyás Horváth (Budapest University of Technology and Economics) for their invaluable help during my work. I would like to express my sincere gratitude also to Dr. Erzsébet Filemon for her helpful advices and remarks devoted this work.

References

- [1] STEWART, D., *Proc. Instn. Mech. Engrs.*, (Part I) **180** (15) (1965/66) pp. 371–386.
- [2] GOUGH, V. E. – WHITEHALL, S. G., *Proc. 9th Int. Tech. Congr. F.I.S.I.T.A.*, May 1962, Instn Mech. Engrs. 117.
- [3] HUNT, K. H., *Kinematic Geometry of Mechanisms*, Clarendon Press, Oxford, 1978.
- [4] LEE, K. – SHAH, D. K., Kinematic Analysis of a Three Degree of Freedom In-Parallel Actuated Manipulator, *Proc. IEEE International Conference on Robotics and Automation*, **1** (1987), pp. 345–350.
- [5] SONG, S. M. – ZHANG, M. D., A Study of Reaction Force Compensation Based on Three-Degree-of-Freedom Parallel Platform, *J. Robot. Syst.*, **12** No. 12, (1995), pp. 783–794.
- [6] SOKOLOV, A., A New Theoretical Approach for the Kinematics and Dynamics of 3-DOF Positioning Parallel Manipulator, 2003, Ph.D. Theses, Lausanne, EPFL.
- [7] BRONSTEJN, I. N. – SZEMENDJAEV, K. A., Szpravocsnik po matematike dlja inzsenerov i ucsacsihszja vuzov, (13-e izd. ispravlennoe) M. Nauka, Gl. Red. Fiz-mat Lit. 1986 –498 c.
- [8] FU, K. S. – GONZALEZ, R. C. – LEE, C. S. G., *Robotics: Control, Sensing, Vision and Intelligence*, pp. 37–40., Mir, Moscow (in Russian), 1989 (Original: McGraw-Hill, Inc.1987).
- [9] LUNG-WEN TSAI, *Robot Analysis: the Mechanics of Serial and Parallel Manipulators*, John Wiley & Sons, Inc., 1999.
- [10] PINTER, J., *Global Optimization in Action. Continuous and Lipschitz Optimization: Algorithms, Implementations and Applications*, 1996 Kluwer Academic Publishers, pp. 243–249.

- [11] GABLONSKY, J. M., An Implementation of the DIRECT Algorithm, Technical Report CRSC-TR98-29, Center for Research in Scientific Computation, North Carolina State University, Raleigh, NC 1998.
- [12] DASGUPTAA, B. – MRUTHYUNJAYA, T. S., The Stewart Platform Manipulator: A Review, *Mechanism and Machine Theory* **35** (2000) pp. 15–40.

Appendix 1

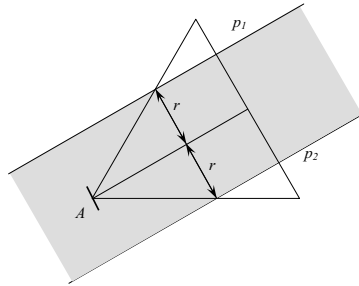


Fig. A.1. Constraints imposed by first R-P-S chain (top view)

Appendix 2

$$\begin{aligned}
 X_a &= X + \begin{bmatrix} \cos \varphi \cos \theta & \cos \varphi \sin \theta \sin \psi - \sin \varphi \cos \psi & \cos \varphi \sin \theta \cos \psi + \sin \varphi \sin \psi \end{bmatrix} \\
 &\quad \times \begin{bmatrix} 0 \\ -\frac{\sqrt{3}r}{2} \\ -\frac{r}{2} \end{bmatrix} \\
 X_b &= X + \begin{bmatrix} \cos \varphi \cos \theta & \cos \varphi \sin \theta \sin \psi - \sin \varphi \cos \psi & \cos \varphi \sin \theta \cos \psi + \sin \varphi \sin \psi \end{bmatrix} \\
 &\quad \times \begin{bmatrix} 0 \\ 0 \\ r \end{bmatrix} \\
 X_c &= X + \begin{bmatrix} \cos \varphi \cos \theta & \cos \varphi \sin \theta \sin \psi - \sin \varphi \cos \psi & \cos \varphi \sin \theta \cos \psi + \sin \varphi \sin \psi \end{bmatrix} \\
 &\quad \times \begin{bmatrix} 0 \\ \frac{\sqrt{3}r}{2} \\ -\frac{r}{2} \end{bmatrix}
 \end{aligned}$$

$$Y_a = Y + \begin{bmatrix} \sin \varphi \cos \theta & \sin \varphi \sin \theta \sin \psi + \cos \varphi \cos \psi & \sin \varphi \sin \theta \cos \psi - \cos \varphi \sin \psi \end{bmatrix} \\ \times \begin{bmatrix} 0 \\ -\frac{\sqrt{3}r}{2} \\ -\frac{r}{2} \end{bmatrix}$$

$$Y_b = Y + \begin{bmatrix} \sin \varphi \cos \theta & \sin \varphi \sin \theta \sin \psi + \cos \varphi \cos \psi & \sin \varphi \sin \theta \cos \psi - \cos \varphi \sin \psi \end{bmatrix} \\ \times \begin{bmatrix} 0 \\ 0 \\ r \end{bmatrix}$$

$$Y_c = Y + \begin{bmatrix} \sin \varphi \cos \theta & \sin \varphi \sin \theta \sin \psi + \cos \varphi \cos \psi & \sin \varphi \sin \theta \cos \psi - \cos \varphi \sin \psi \end{bmatrix} \\ \times \begin{bmatrix} 0 \\ \frac{\sqrt{3}r}{2} \\ -\frac{r}{2} \end{bmatrix}$$

$$Z_a = Z + \begin{bmatrix} -\sin \theta & \cos \theta \sin \psi & \cos \theta \cos \psi \end{bmatrix} \\ \times \begin{bmatrix} 0 \\ -\frac{\sqrt{3}r}{2} \\ -\frac{r}{2} \end{bmatrix}$$

$$Z_b = Z + \begin{bmatrix} -\sin \theta & \cos \theta \sin \psi & \cos \theta \cos \psi \end{bmatrix} \\ \times \begin{bmatrix} 0 \\ 0 \\ r \end{bmatrix}$$

$$Z_c = Z + \begin{bmatrix} -\sin \theta & \cos \theta \sin \psi & \cos \theta \cos \psi \end{bmatrix} \\ \times \begin{bmatrix} 0 \\ \frac{\sqrt{3}r}{2} \\ -\frac{r}{2} \end{bmatrix}$$

Appendix 3

$$\text{Theta} = \arctan\left(\frac{-(-2*X-3*R*\tan(\text{Psi})+2*Y*\tan(\text{Psi})-2*X*\tan(\text{Psi})^2+2*Y*\tan(\text{Psi})^3+R*\tan(\text{Psi})^3)/(R*\tan(\text{Psi})*(-3+\tan(\text{Psi})^2)),2*\text{RootOf}(X^2+2*X^2*\tan(\text{Psi})^2+2*Y^2*\tan(\text{Psi})^4+Y^2*\tan(\text{Psi})^2+Y^2*\tan(\text{Psi})^6+X^4*2*\tan(\text{Psi})^4-2*R*\tan(\text{Psi})^4*Y-3*R*\tan(\text{Psi})^2*Y+Y*\tan(\text{Psi})^6*R-X*\tan(\text{Psi})^5*R-2*X*\tan(\text{Psi})^5*Y+3*X*R*\tan(\text{Psi})+2*X*R*\tan(\text{Psi})^3-4*X*Y*\tan(\text{Psi})^3-2*X*Y*\tan(\text{Psi})+_Z^2)/((-3+\tan(\text{Psi})^2)*\tan(\text{Psi})*R)}{R}\right),$$

$$Z = 1/2*(X*\tan(\text{Psi})^2*R+2*X*\tan(\text{Psi})^2*Y-2*R*Y*\tan(\text{Psi})-2*X^2*\tan(\text{Psi})+2*Y^2*\tan(\text{Psi})-X*R-2*X*Y)*\text{sqrt}((\tan(\text{Psi})^2+1)/$$

$$\begin{aligned}
 & (\tan(\Psi)^2) * \tan(\Psi) / \text{RootOf}(X^2 + 2 * X^2 * \tan(\Psi)^2 + \\
 & 2 * Y^2 * \tan(\Psi)^4 + Y^2 * \tan(\Psi)^2 + Y^2 * \tan(\Psi)^6 + X^2 * \tan(\Psi)^4 - \\
 & 2 * R * \tan(\Psi)^4 * Y - 3 * R * \tan(\Psi)^2 * Y + Y * \tan(\Psi)^6 * R - \\
 & X * \tan(\Psi)^5 * R - 2 * X * \tan(\Psi)^5 * Y + 3 * X * R * \tan(\Psi) \\
 & + 2 * X * R * \tan(\Psi)^3 - 4 * X * Y * \tan(\Psi)^3 - 2 * X * Y * \tan(\Psi) + _Z^2),
 \end{aligned}$$

Appendix 4

$$\begin{aligned}
 X1 = & (-1.0) * A3 / (4.0 * A4) - \text{sqrt}(\text{pow}(A3, 2.0) / (4.0 * \text{pow}(A4, 2.0)) - \\
 & (2.0 * A2) / (3.0 * A4) + (\text{pow}(2.0, (1./3.)) * (\text{pow}(A2, 2.0) - \\
 & 3.0 * A1 * A3 + 12.0 * A0 * A4))) / (3.0 * A4 * \text{pow}(2.0 * \text{pow}(A2, 3.0) - \\
 & 9.0 * A1 * A2 * A3 + 27.0 * A0 * \text{pow}(A3, 2.0) + 27.0 * \text{pow}(A1, 2.0) * A4 - \\
 & 72.0 * A0 * A2 * A4 + \text{sqrt}(-4.0 * \text{pow}(\text{pow}(A2, 2.0) - 3.0 * A1 * A3 + 12.0 * A0 * A4, 3.0) + \\
 & \text{pow}(2.0 * \text{pow}(A2, 3.0) - 9.0 * A1 * A2 * A3 + 27.0 * A0 * \text{pow}(A3, 2.0) + \\
 & 27.0 * \text{pow}(A1, 2.0) * A4 - 72.0 * A0 * A2 * A4, 2.0)), (1./3.))) + \\
 & \text{pow}(2.0 * \text{pow}(A2, 3.0) - 9.0 * A1 * A2 * A3 + 27.0 * A0 * \text{pow}(A3, 2.0) + \\
 & 27.0 * \text{pow}(A1, 2.0) * A4 - 72.0 * A0 * A2 * A4 + \text{sqrt}(-4.0 * \text{pow}(\text{pow}(A2, 2.0) \\
 & - 3.0 * A1 * A3 + 12.0 * A0 * A4, 3.0) + \text{pow}(2.0 * \text{pow}(A2, 3.0) - 9.0 * A1 * A2 * A3 + \\
 & 27.0 * A0 * \text{pow}(A3, 2.0) + 27.0 * \text{pow}(A1, 2.0) * A4 - 72.0 * A0 * A2 * A4, 2.0)), (1./3.))) / \\
 & (3.0 * \text{pow}(2.0, (1./3.)) * A4) / (2.0 * \text{sqrt}(\text{pow}(A3, 2.0) / (2.0 * \text{pow}(A4, 2.0)) - \\
 & (4.0 * A2) / (3.0 * A4) - (\text{pow}(2.0, (1./3.)) * (\text{pow}(A2, 2.0) - 3.0 * A1 * A3 + \\
 & 12.0 * A0 * A4))) / (3.0 * A4 * \text{pow}(2.0 * \text{pow}(A2, 3.0) - 9.0 * A1 * A2 * A3 + \\
 & 27.0 * A0 * \text{pow}(A3, 2.0) + 27.0 * \text{pow}(A1, 2.0) * A4 - 72.0 * A0 * A2 * A4 + \\
 & \text{sqrt}(-4.0 * \text{pow}(\text{pow}(A2, 2.0) - 3.0 * A1 * A3 + 12.0 * A0 * A4, 3.0) + \text{pow}(2.0 * \text{pow}(A2, 3.0) - \\
 & 9.0 * A1 * A2 * A3 + 27.0 * A0 * \text{pow}(A3, 2.0) + 27.0 * \text{pow}(A1, 2.0) * A4 - \\
 & 72.0 * A0 * A2 * A4, 2.0)), (1./3.))) - \text{pow}(2.0 * \text{pow}(A2, 3.0) - \\
 & 9.0 * A1 * A2 * A3 + 27.0 * A0 * \text{pow}(A3, 2.0) + 27.0 * \text{pow}(A1, 2.0) * A4 - 72.0 * A0 * A2 * A4 + \\
 & \text{sqrt}(-4.0 * \text{pow}(\text{pow}(A2, 2.0) - 3.0 * A1 * A3 + 12.0 * A0 * A4, 3.0) + \text{pow}(2.0 * \text{pow}(A2, 3.0) - \\
 & 9.0 * A1 * A2 * A3 + 27.0 * A0 * \text{pow}(A3, 2.0) + 27.0 * \text{pow}(A1, 2.0) * A4 - \\
 & 72.0 * A0 * A2 * A4, 2.0)), (1./3.))) / (3.0 * \text{pow}(2.0, (1./3.)) * A4) - \\
 & (-\text{pow}(A3, 3.0) / \text{pow}(A4, 3.0)) + (4.0 * A2 * A3) / \text{pow}(A4, 2.0) - \\
 & (8.0 * A1) / A4 / (4.0 * \text{sqrt}(\text{pow}(A3, 2.0) / (4.0 * \text{pow}(A4, 2.0)) - (2.0 * A2) / (3.0 * A4) + \\
 & (\text{pow}(2.0, (1./3.)) * (\text{pow}(A2, 2.0) - 3.0 * A1 * A3 + 12.0 * A0 * A4))) / (3.0 * A4 * \text{pow}(2.0 * \text{pow}(A2, 3.0) - \\
 & 9.0 * A1 * A2 * A3 + 27.0 * A0 * \text{pow}(A3, 2.0) + 27.0 * \text{pow}(A1, 2.0) * A4 - 72.0 * A0 * A2 * A4 + \\
 & \text{sqrt}(-4.0 * \text{pow}(\text{pow}(A2, 2.0) - 3.0 * A1 * A3 + 12.0 * A0 * A4, 3.0) + \text{pow}(2.0 * \text{pow}(A2, 3.0) - \\
 & 9.0 * A1 * A2 * A3 + 27.0 * A0 * \text{pow}(A3, 2.0) + 27.0 * \text{pow}(A1, 2.0) * A4 - 72.0 * A0 * A2 * A4, 2.0)), (1./3.))) + \text{pow}(2.0 * \text{pow}(A2, 3.0) - \\
 & 9.0 * A1 * A2 * A3 + 27.0 * A0 * \text{pow}(A3, 2.0) + 27.0 * \text{pow}(A1, 2.0) * A4 - 72.0 * A0 * A2 * A4 + \\
 & \text{sqrt}(-4.0 * \text{pow}(\text{pow}(A2, 2.0) - 3.0 * A1 * A3 + 12.0 * A0 * A4, 3.0) + \text{pow}(2.0 * \text{pow}(A2, 3.0) - \\
 & 9.0 * A1 * A2 * A3 + 27.0 * A0 * \text{pow}(A3, 2.0) + 27.0 * \text{pow}(A1, 2.0) * A4 - 72.0 * A0 * A2 * A4, 2.0)), (1./3.))) / (3.0 * \text{pow}(2.0, (1./3.)) * A4) / 2.
 \end{aligned}$$

Appendix 5

Numerical Solution

As it is described in the mathematical literature [7], if the continuous functions $f_1(x)$, $f_2(x)$, \dots , $f_n(x)$ of n independent variables $x = (x_1, x_2, \dots, x_n)$ are defined in the common domain of definition $D \subseteq \mathbb{R}^n$, and the vector $x_N \in D$ exists, and for this vector $f_j(x_N) = 0$ ($j = 1 \dots n$), then x_N is called *solution-vector* of the non-linear equation system $f(x) = 0$:

$$(f(x)) = (f_1(x), f_2(x) \dots f_n(x))^T$$

The determination of this solution is described in the following:

1. Linearization. Non-linear representation of $f(x)$ is changed by the appropriate linear mapping $L(x) = Ax + b$ (where A is the matrix of $n \times n$ dimension). So, if some special conditions are satisfied, the solution x_L of the system $L(x) = 0$ will be a good estimation to x_N .

Newton–Kantorovich Method (Linearization Using Taylor Series)

Let $x^{(0)}$ be the initial estimation of x_N , and differentiable at least once in D ; then

$$f(x) = f(x^{(0)}) + \left. \frac{\partial(f_1, f_2, \dots, f_n)}{\partial(x_1, x_2, \dots, x_n)} \right|_{x=x^{(0)}} (x - x^{(0)}) + R(x).$$

Discarding the remainder term $R(x)$

$$L(x) = A(x - x^{(0)}) + f(x^{(0)}),$$

where A is the Jacobi matrix

$$\left. \frac{\partial(f_1, f_2, \dots, f_n)}{\partial(x_1, x_2, \dots, x_n)} \right|_{x=x^{(0)}}.$$

Let decide that A is non-degenerated matrix. So, the system $y = f(x)$ is uniquely solvable in the vicinity of $x^{(0)}$.

According to the previous explanation, the Newton–Kantorovich method is described by the following schema:

1. The choice of initial estimation $x^{(0)}$ of x_N .
2. The evaluation of $A(x^{(0)})$ matrix.
3. The solution $z^{(1)}$ of the system

$$A(x^{(0)})z + f(x^{(0)}) = 0 \tag{A5.1}$$

gives a new estimation of $x^{(1)} = x^{(0)} + z^{(1)}$, and the process should be repeated until the difference $z^{(j)}$ will satisfy the required accuracy.

Appendix 6

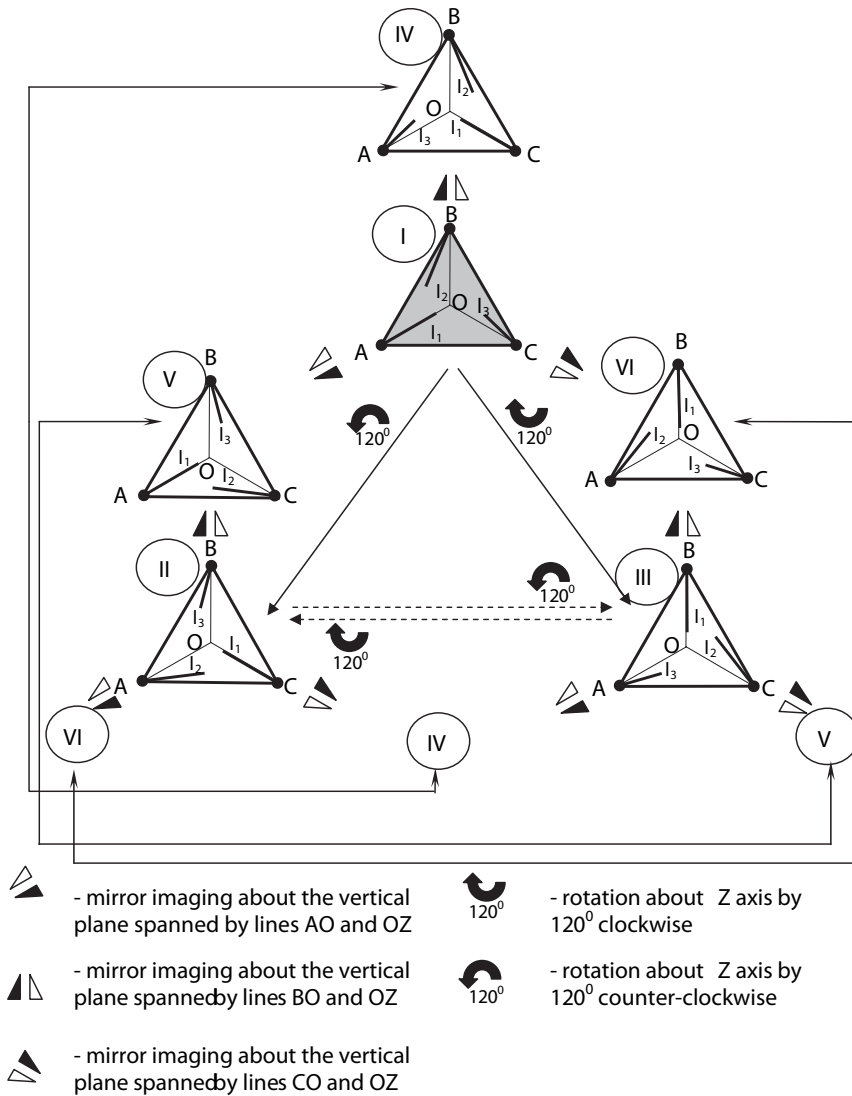


Fig. A.2. Configurations received by means of transformations in a Cartesian space